Title
VSP Analysis at Long Valley Caldera, Eastern California

Author
Gritto, Roland

Publication Date
1999-06-28

LBNL-39108

ERNEST ORLANDO LAWRENCE
BERKELEY NATIONAL LABORATORY

VSP Analysis at Long Valley Caldera, Eastern California

Roland Gritto, Art E. Romero,
and Thomas M. Daley

Earth Sciences Division

June 1999

DISCLAIMER

LBNL-39108

VSP Analysis at Long Valley Caldera, Eastern California

Roland Gritto, Art E. Romero, and Thomas M. Daley

Earth Sciences Division
Ernest Orlando Lawrence Berkeley National Laboratory
University of California
Berkeley, California 94720

June 1999

This work was supported by the Director, Office of Energy Research, Division of Basic Energy Sciences, Engineering, and Geosciences, of the U.S. Department of Energy under Contract No. DE-AC03-76SF00098.

VSP Analysis at Long Valley Caldera, Eastern California

Roland Gritto[1,2], Art E. Romero[3] and Thomas M. Daley [1]

Numerous scientific studies have focused on the Long Valley Caldera in recent years, encouraged by indications of renewed volcanic activity and a resurgent dome. A deep ($\sim$ 2 km) scientific well, drilled by the Department of Energy (DOE Exploratory Well LVF 51-20), provided an opportunity to perform a vertical seismic profile (VSP) within the resurgent dome. We have acquired and analized the VSP for P-wave and S-wave velocity and reflectivity. It did prove difficult to obtain good quality seismic data over the entire well depth, with S-waves being strongly attenuated. However, we were able to interpret both velocity and reflectivity. First arrival travel times give velocity and Poisson's Ratio and later arriving energy provides reflectivity information. A transition from post caldera rhyolites and unwelded tuff to welded Bishop tuff is marked by a velocity increase at about 820 m and reflections between 600 m and 700 m. The Bishop tuff was intersected by the well at 620 m. Fracture zones, possibly related to geothermal activity, are inferred from Poisson's ratio variations at depth of about 700 m and 930 m and interpreted for fluid/gas saturation. Reflectivity between 1 km and 1.6 km which is not associated with lithologic changes, is interpreted as being associated with caldera faulting. We found no evidence of strong reflections from below the well to depths of 2-5 km, indicating the absence of a large scale magma chamber at these crustal depths. Despite the difficulties of seismic recording in heterogeneous fractured volcanic rocks, the application of the VSP method allowed direct measurement of seismic properties which are interpreted for structure within the resurgent dome and can be used in other regional seismic studies.

[1]Center for Computational Seismology, Lawrence Berkeley National Laboratory, Berkeley, California.

[2]Seismological Laboratory, University of California, Berkeley.

[3]Exxon Production Research Company, Houston, Texas.

Introduction

The Long Valley Caldera (LVC), located on the eastern side of the Sierra Nevada Mountains in California, has been the subject of numerous geophysical studies over the last 20 years. In addition to purely scientific interest in caldera structures, the possibility of renewed volcanic activity caused noteable public concern in nearby communities such as Mammoth Lakes (California) in the 1980's. Additionally, there is geophysical interest in the exploration for geothermal energy from steam producing wells located within the caldera.

As part of a Department of Energy (DOE) drilling program, the Lawrence Berkeley National Laboratory (LBNL) conducted a Vertical Seismic Profile (VSP) experiment within the caldera. The VSP experiment was designed to acquire both P-wave and S-wave velocities over the drilled interval and to gather reflectivity information about structures within the drilled interval. Additionally, it was hoped that the VSP could "look ahead" and identify reflective structures below the well such as a distinct magma chamber.

Background

Long Valley caldera is a Quaternary volcanic structure located at the intersection of the Sierra Nevada frontal fault escarpment and the western margin of the Basin and Range tectonic province. The geologic development of the region has been well documented by *Bailey et al.* [1976] and *Bailey* [1989]. These studies traced the formation of the 32 km by 17 km caldera from a voluminous ash eruption of a silicic volcano 760,000 years ago. The cataclysmic eruption ejected about 650 km^3 of rhyolitic ash that became the Bishop tuff. Subsequent volcanism occurred in several episodes within the caldera and formed the resurgent dome. The most recent eruption occurred about 200 years ago at the Mono-Inyo craters. These craters form a chain of eruptive centers extending from the western moat of the caldera northward to the Mono Basin. Fig. 1 presents a schematic view of the geology of the LVC region.

In 1980, strong evidence of renewed magma movement became apparent following a series of large magnitude earthquake sequences accompanied by rapid surface uplift [*Ryall and Ryall,* 1981; *Savage et al.,* 1987]. Proposed models to explain the deformation include dike intrusion and magma inflation beneath the caldera at shallow to mid-crustal depths [*Rundle and Whitcomb,* 1984; *Savage and Cockerham,* 1984; *Vasco et al.,* 1988]. Other geophysical studies have suggested the existence of a magma chamber beneath the resurgent dome (reviews are presented in *Hill et. al.,* 1985a and *Goldstein and Stein,* 1988). *Hill* [1976] and *Hill et al.,* [1985b] showed possible seismic reflectors at 7 km - 8 km depth beneath the western margin of the resurgent dome as the top of a magma chamber. Other studies interpreted deeper reflectors to be the bottom of the magma chamber [*Luetgert and Mooney,* 1985; and *Zucca et al.,* 1987]. *Sanders* [1984], [1993] and *Ponko and Sanders* [1994] mapped shear-wave attenuation zones as possible magma bodies between 5 km and 8 km depth beneath the west moat and the resurgent dome. *Dawson et al.* [1990] and *Steck and Prothero* [1991], utilizing teleseismic P-wave delays, found a low-velocity body between 7 km and 20 km depth at the western and central region of the caldera.

In contrast, several studies do not support the presence of a sizable magma body at shallow to mid-crustal depth beneath LVC. The tomographic study by *Kissling* [1988] found no evidence for the presence of a magma body beneath LVC. *Romero et al.* [1993] did not detect significant S-wave velocity anomaly, although a diffuse zone of reduced velocity persists to a depth of about 8 km. These lower velocities may be related to hydrothermal alteration and/or extensive fractures. *Hauksson* [1988] suggested that the observed S-wave shadowing found by *Sanders* [1984] could be explained by radiation pattern effects. *Black et. al.* [1991], employing a new migration algorithm, concluded that the events previously interpreted as reflections from a magma chamber were most probably reflections from the faults of the caldera ring fracture system.

The conflicting results are caused by complex geological structure beneath LVC. The collapsed caldera together with the cycles of volcanic eruptions has created a crust highly fractured with little evidence of lateral homogeneity. Additionally, it was found that the topmost layer, the non-welded Bishop tuff, acts as a highly attenuating medium for elastic wave propagation. However, most of the seismological investigations were performed as surface reflection experiments, facing the difficulties of energy propagation through the non-welded tuff, and furthermore, interpreting the scattered reflected energy on the basis of the assumptions of laterally homogeneous media, with little knowledge about the actual subsurface velocities.

In an attempt to resolve these conflicting results,

the Department of Energy's Basic Energy Science and Continental Scientific Drilling programs completed a deep exploratory well (named Long Valley Federal 51-20) within LVC to test for the presence of recent magma intrusions. The well was located within the center of the resurgent dome (Fig. 1). LBNL collected a Vertical Seismic Profile after the second phase of drilling in September 1992. Our study within the DOE LVC project is the only deep VSP experiment performed at LVC to date. Compared to surface seismic recordings, application of the VSP method within a deep borehole provides a better opportunity to understand rock properties in the near-well region, and to tie seismic reflectivity to lithologic or hydrologic properties. Recording at depth has the potential advantages that waves excited at the surface have to propagate through the highly attenuating surface layers only once, and that recording in a quieter environment, with better signal to noise ratio, will improve the ability to detect reflections from beneath the well bottom. With the VSP, we can measure seismic velocity as a function of depth to the deepest recording and compare the resulting velocity and Poisson's ratio model to other seismological studies in the region. Our study also aims to search for reflections from within the depth interval of the borehole and possibly from below. This information could be used in planning future drilling phases.

Data Acquisition and Processing

Data Acquisition

Figure 1 shows the site of the exploratory well, with the geological setting of LVC. Two source positions were selected with their locations 165 m and N65°E (near offset), and 1524 m and N180°S (far offset) relative to the well (not indicated in Figure 1 for scaling reasons). Closer source locations were tried for the near offset, but they generated high amplitude tube waves which degraded data quality. The sources were P- and S-wave vibroseis trucks exciting sweeps 12 seconds long with frequency content of 10 Hz to 58 Hz. Each sweep had a 6 s listen time. Five to ten sweeps were recorded for each source receiver pair depending on the signal to noise ratio at each receiver location. The data were acquired at depths between 550 m and 2075 m at 15 m depth intervals. The receiver was a three-component (vertical and two orthogonal horizontals), high-temperature, hydraulic wall-locking borehole seismometer. The data discussed in this paper was the near offset part of a larger data acquisition effort described in Table 1. The far offset portions of the data had less sampling and proved difficult to interpret because of presumed lateral heterogeneity. The data was recorded uncorrelated with field correlation used for quality control.

Data Processing

The data processing can be divided into several steps as shown in Figure 2. The editing process reduced the field data into several subsets according to the source locations, source types and receiver components. The reduction consisted of editing noise bursts that appear in the raw traces (Figure 3a), followed by a stack of the 5-10 source sweeps per receiver location to improve the signal to noise ratio. Figure 3a shows a typical sequence of unprocessed data revealing 10 groups of 3 geophone traces next to the source sweep for the same receiver location at 2075 m depth. The stacking procedure was followed by correlating the recorded traces with the source sweep to recover the bandlimited impulse source response. The original recording time consisted of 18 s (12 s sweep time plus 6 s listening time) which was reduced to 6 s of data after correlation. The stacked and correlated data are presented in Figure 3b. Direct P- and S-waves as well as tube waves are distinguished by different moveouts. Strong tube waves, apparent throughout the data set, are generated by conversion of ground roll and body waves at the borehole. Throughout the study, the tube waves complicated the detection of possible reflections from features below the well bottom. A numerical rotation of the geophone components, using the P-wave first arrival particle motion, was performed to provide a consistent coordinate system, thereby maximizing the depth coherency of P- and S-waves on the three components. The analysis of travel time and reflectivity was performed on the rotated geophone components.

Velocity Analysis

The data editing was followed by the determination of the first arrival times for the direct P- and S-waves from the near offset site. Noticeable scatter in arrival times for the first 12 traces was observed. The complex shallow lithology down to about 730 m depth, consisting of mainly post caldera volcanics, pyroclastic deposits, and non-welded tuff, could complicate the determination of the arrival time for both wave types by local scattering. Poor coupling of the casing to the lithology and multistring casing could both be factors in the scatter of the arrival time. The P-

wave energy decreases gradually with depth, whereas a sudden drop in S-wave energy in the bottom section of the well reduces the reliability of the arrival times of the shear waves in this depth range (Figure 3b).

Assuming straight ray geometry between the source and the receiver positions in the well, interval velocities for every receiver location are computed. In order to eliminate local velocity anomalies due to poor quality S-wave time picks, we average the velocity with a 20 point running window of 300 m length. The velocity depth profile for the near offset is shown in Figure 4a. The shortened depth range is caused by the averaging process which decreases the profile length by 150 m at both ends. The scatter in the S-wave velocity between 1350 m and 1925 m is related to the poor signal to noise ratio in the seismograms which complicated the picking of the direct S-wave arrivals. The Poisson's ratio presented in Figure 4b is calculated from V_p and V_s, and therefore, partly reflects the uncertainty in the 1370 m to 1920 m depth range. Whereas low values manifested by single outlyers between 1500 m and 1850 m seem doubtful, low readings at the depth around 900 m appear significant as they are supported by several data points in a zone of relatively good data quality.

Reflection Analysis

The travel times of the direct waves were used to apply static corrections to the downgoing P and S-wavefields and to align their first arrivals uniformly at a predefined time. Once the data are corrected for the direct travel time delays, a wavefield separation of downgoing and upcomming (reflected) arrivals is performed by transformation into the frequency-wavenumber (f-k) domain. The downgoing energy appears centered around the $k = 0\ m^{-1}$ wavenumber for all frequencies. We then apply a narrow velocity filter to exclude this part of the wavefield without rejecting too much energy in the f-k domain. Minimizing the energy of the downgoing wavefield facilitates the identification of possible reflections in the data. The same procedure was applied to remove tube wave energy. However, because of the large amplitude of tube waves and their multiple arrivals in most parts of the seismic traces, a complete removal was not achieved.

The final step consists of a VSP-CDP mapping of the data from time to depth scale [*Dillon and Thomson,* 1984]. The mapping is based on the assumption of horizontal layering with laterally uniform velocities. Therefore, a simplified layered model was derived from the travel time picks in order to facilitate the VSP-CDP mapping. The assumption of a horizontally layered, laterally uniform velocity model is questionable, however, it is probably acceptable as the horizontal source offset is only 165 m. Because of this limitation in the velocity model, and the single source position at the far offset, a VSP-CDP mapping for the far offset data was not attempted.

Interpretation

Interpretation of the velocity data

The variation of the interval velocity with depth is given in Figure 4a. It exhibits a good correspondence with lithology and is consistent with the upper crustal structure determined from a refraction survey by *Hill et al.,* [1985b]. Above 700 m, a P-wave velocity of about 3100 m/s is obtained for the fractured post caldera volcanics consisting of rhyolite and basalt lava flows, and non-welded Bishop tuff. The velocity significantly increases to 3650 m/s between 750m and 800 m which probably marks the transition to welded Bishop tuff. Within this formation it increases slowly with depth, except for a sharp jump at 950 m. Although it is still unclear, it may have some relation to the overlaying low velocity zone which could be attributed to a gas-filled fractured zone (discussed below). A small velocity increase around 1150 m may indicate the presence of a fault. Between 1550 m and 1750 m, the velocities decrease by approximately 300 m/s wheres it increases below this interval again. The decrease at the base of the Bishop tuff could be attributed to the presence of a breccia stratum consisting of fragments of the Bishop tuff and the metasedimentary basement below [*Finger and Jacobson,* 1992]. The increase to values above 4500 m/s below 1800 m denotes the transition to the crystalline basement which was encountered at a depth of 2025 m within the borehole. The S-wave velocity structure generally shows those variations seen in the P-wave, with a smaller velocity gradient at depth. It should be emphasized again that the interval velocity produces velocity values averaged over 300 m, and therefore, they do not represent the exact geological situation encountered at a single depth in the borehole.

Changes in the observed Poison ratio ($\propto V_p/V_s$) (Fig. 4b), along with the P and S velocities, indicate changes in the mechanical properties of the rocks in situ. In LVC, V_p/V_s variation can be explained in terms of fluid saturation. Studies have shown that over-saturation increases the effective V_p/V_s while under-saturation (dry or gas-filled fractures) decreases

it [*Toksöz, et al.,* 1976; and *Gregory,* 1976]. The relatively high V_p/V_s ratio between 700 m and 750 m indicates the presence of fluid saturated fractures. At these depths, several zones of lateral fluid flow have been delineated by *Sorey et al.* [1991].

A low V_p/V_s ratio around 920 m may suggest the presence of under-saturated fractures with some gas content, perhaps a combination of steam and non-condensable gases. This anomaly may indicate the presence of a confined steam zone caused by geothermal fluid withdrawal from several production wells nearby. A pervasive low V_p/V_s ratio has been observed in the developing steam cap above the producing zone in The Geysers, California, due to a long history of geothermal fluids withdrawal *Romero et al.,* [1995]. Relatively high V_p/V_s are obtained between 1450 m and 2000 m. This high anomaly has been previously observed in a 3-D velocity inversion by *Romero et al.,* [1993] and interpreted in terms of increased fluid saturation possibly due to the injection of geothermal fluids within the area.

Interpretation of the reflection data

The VSP-CDP mapping produced results that are consistent with the lithology derived from several previous studies. In particular the geology of the upper 2 km is well constrained by the presence of numerous boreholes in the region. The results of the mapping are presented in Figure 5. The figure represents band pass depth filtered images of CDP maps, stacked over all traces to enhance the reflectivity for the near offset. The depth filter produced a resolving wavelength between 35 m and 100 m. In the following, we will first point out reflections visible in the seismograms that coincide in depth with horizons penetrated by the borehole.

A series of reflections (No.1, Figure 5a) centered between 600 m and 700 m marks the complicated shallow lithology consisting of post caldera volcanics in the form of flows and domes, and pyroclastic deposits consisting mainly of non-welded Bishop tuff *Bailey et al.,* [1976]. The reflections may also arise from the interface between the post caldera volcanics and the welded Bishop tuff which was intersected at a depth of 620 m by the well [*Finger and Jacobsen,* 1992]. The absence of this reflection in the S-wave data is due to its poor quality in the upper 200 m of the recording interval. About 800 m depth, a reflection (No. 2, Figure 5b) is apparent in the S-wave data that correlates with the encounter of a dike-like intrusion in the borehole. Between 1700 m and 1800 m depth, a P- and S-wave reflection coincide with the top of a 90 m thick breccia layer encountered by the borehole (No. 3, Figure 5a, 5b). The extent of the layer may cause the broadening of the reflection pulse. The caldera basement was encountered by the borehole as a transition from volcanic to metamorphic rocks. The first metamorphic layer consist of metamorphic volcanic rocks at a depth of 1800 m and 90 m thickness. Accordingly, weak reflections around 1900 m can be seen in both P- and S-waves (No. 4, Figure 5a, 5b). The basement follows with a transition to metamorphic sediments (the Mt. Morrison formation) at a depth of 2025 m, supported by a strong reflection in the P-wave (No. 5, Figure 5a), whereas no clear reflection is evident in the S-wave data (No. 5, Figure 5b)

For the far offset VSP data, the CDP mapping based on a single source position and a horizontally continuous 1-d velocity model provides questionable insight into the geologically complicated setting of a volcanic caldera. While the general assumption of horizontally layered bedding can be a valid approximation considering the process of volcanic deposition, post volcanic tectonic activity will disturb this layered sequence and juxtaposed geological units can be expected. In this sense, it is important to match the reflections in the CDP map with the depth of the associated layers encountered in the borehole. The relatively good match between the near offset seismic and borehole data indicates that the assumption of horizontal layering for the main geological units and their estimated P- and S-wave velocities seem reasonable for this short offset survey.

Various geologic studies revealed an abundance of faults evident in this area *Bailey,* [1989]. The majority of these faults are normal faults, although the actual degree of dip is mostly unknown. Therefore, it is impossible to map these faults accurately based on the single offset data set presented in this study, as a reflected wave from these faults, at a given time in the traces, could be incident from any azimuth. Additionally, the 1-d velocity model would estimate an intercept of the fault with the borehole at a depth shallower than the true intercept. Furthermore, no apparent faults were intersected in the borehole during the drilling process. Thus our interpretation of possible reflections of faults around the well is simply suggestive of potential out-of-plane reflectivity.

Three reflections are visible in the data that do not correlate with the geological data encountered in the well. These are a reflector just below 1000 m in both P- and S-wave (No. 6, Figure 5a, 5b), a series

of arrivals between 1300 m and 1400 m (P-wave) and around 1300 m (S-wave) (No. 7, Figure 5a, 5b), and finally a strong reflection around 1500 m in both P- and S-wave data (No. 8, Figure 5a, 5b). If these reflections originated at out-of-plane faults at some distance form the borehole the zero offset assumption of vertical wave incidence is no longer valid and it can be expected that the arrival times between P- and S-waves differ, because the path of propagation will depend on the velocity model. This is supported by the variation in depth of these reflections between Figure 5a and 5b. However, the strong reflection at about 1500 m depth coincides with a decrease in P- and S-wave velocities as indicated in Figure 4a, and therefore may indicate lithological changes in the vicinity of the borehole.

These reflections may be attributed to faults mapped by *Bailey* [1989] as evident in the crossection in Figure 6. These faults belong to the medial-graben system striking in NW-SE direction. Although the location of the well is superimposed on the cross-section of Figure 6, its true location is farther to the West (into the plane of the crossection). Since the faults are presumed to dip steeply towards the West (although the true angle is not known), they probably do not intersect the borehole as shown in this projection, but cross the well location at a depth below the well bottom. This assumption is supported by the absence of any apparent fault in the well. However, as the fault dips west, energy reflecting off its plane is recorded in the well and the 1-D mapping procedure locates the arrivals at a depth within the well. At this point, with the present data, we cannot determine whether this energy is reflected off dipping faults or off other out-of-plane reflectors that do not cross the well.

Apart from the structures discussed above, no clear reflections were evident beneath the bottom (to a depth of about 2-5 km), thus doubting the existence of a distinct magma chamber at these crustal depths. Figure 7 presents the f-k filtered reflection seismograms for the P and S-wave data. Most of the energy apparent in the sections is multiple reflected tube wave energy that could not be completely eliminated from the data. One possible coherent reflection below the well bottom is indicated by the white arrow in the S-wave data after a time of 1.5 s. Assuming a horizontal reflector, the depth can be estimated as 2230 m (or $\sim$ 160 m below the well bottom). In contrast, it may be as likely that again, this energy is associated with an out-of-plane reflection. However, we cannot rule out the presence of discrete dike or sill intrusions that do not produce a continuous reflection strong enough to be detected in the seismogram sections.

Conclusion

The Long Valley Caldera, a geologically complex volcanic environment, presents a compelling challenge in analyzing VSP data. Anisotropy and scattering perturb wave field coherency, while strong velocity gradients and laterally varying structures disperse seismic waves in all directions, complicating the separation of the downgoing and upcomming wave fields. Completion procedures (such as multiple casing strings) prevented recording at shallow depths, and may have contributed to tube wave noise. Nevertheless, we were able to obtain P-wave and S-wave velocity structure to nearly 2 km depth, and identify seismic reflections above the well bottom which show correspondence to lithological changes. These changes mark the transition from post caldera rhyolites and unwelded tuff to welded Bishop tuff at about 600 m to 700 m, the intersection of the breccia stratum around 1700 m, and finally the crystaline basement at 2025 m. Fracture zones with possibly varying gas/fluid saturations were detected by velocity variations just below 1000 m. These fracture zones may play a role in shallow geothermal activity. Furthermore, reflections indicate the possible existence of faults at an apparent depth of 1000 m, 1300 m, and 1500 m. However, based on additional work by *Bailey* [1989]it is suggested that the intersections of these faults with the borehole axis lie below the well bottom. At the same time it cannot be ruled out that this energy is reflected by other out-of-plane reflectors. The absence of significant reflections down to 5 km below the well does not support the presence of a distinct magma chamber beneath the resurgent dome.

Acknowledgments The authors are grateful to Don Lippert of Geophysical Measurements Facility (LBNL) for help in data acquisition, and Ernie Majer for project funding. Special thanks to Jamie Rector III for his advice on data processing. This research was supported by the Director, Office of Energy Research, Division of Basic Energy Sciences, Engineering, and Geosciences, of the U.S. Department of Energy under contract DE-AC03-76SF00098. All computations were carried out at the Center for Computational Seismology of the Lawrence Berkeley National Laboratory.

References

Black, R. A., S. J. Deemer, and S. B. Smithson, Seismic reflection studies in Long Valley caldera, California, *J. Geophys. Res., 96,* 4289-4300, 1991.

Bailey, R. A., G. B. Dalrymple, and M. A. Lanphere, Volcanism, structure, and geochronology of Long Valley Caldera, Mono County, California, *J. Geophys. Res., 90,* 725-744, 1976.

Bailey, R. A., Geologic map of Long Valley caldera, Mono-Inyo craters volcanic chain, and vicinity, Eastern California, *USGS MAP I-1933,* 1989.

Dawson, P. B., J. R. Evans, and H. M. Iyer, Teleseismic tomography of the compressional wave velocity structure beneath the Long Valley region, California, *J. Geophys. Res., 95,* 11,021-11,050, 1990.

Dillon, P.B., and R. C. Thomson, Offset source VSP surveys and their image reconstruction, *Geophys. Prosp., 32,* 790-811, 1984.

Finger, J.T., and R. D. Jacobson, Phase II drilling operation at the Long Valley Exploratory Well (LVF 51-20), *SAND92-0531 UC-253* 1992.

Goldstein, N. E., and R. S. Stein, What's new at Long Valley, *J. Geophys. Res., 93,* 13187-13190, 1988.

Gregory, A. R., Fluid saturation effects on dynamic elastic properties of sedimentary rocks, *Geophysics, 41,* 895-921, 1976.

Haukkson, E., Absence of evidence for a shallow magma chamber beneath Long Valley caldera, California, in downhole and surface seismograms, *J. Geophys. Res., 93,* 13251-13264, 1988.

Hill, D. P., Structure of Long Valley caldera from seismic refraction experiments, *J. Geophys. Res., 81,* 745-753, 1976.

Hill, D. P., R. A. Bailey, and A. S. Ryall, Active tectonic and magmatic processes beneath Long Valley Caldera, Eastern California: An overview, *J. Geophys. Res., 90,* 11,111-11,120, 1985a.

Hill, D. P., E. Kissling, J. H. Luetgert, and U. Kradolfer, constraints on the upper crustal structure of the Long Valley-Mono craters volcanic complex, Western California, from seismic refraction measurements, *J. Geophys. Res., 90,* 11,135-11,150, 1985b.

Kissling, E., Geotomography with local earthquake data, *Rev. Geophys., 26,* 659-698, 1988.

Luetgert, J. H., and W. D. Mooney, Crustal refraction profile of Long Valley caldera, California, from the January 1983 Mammoth Lakes earthquake swarm, processes beneath Long Valley Caldera, Eastern California: An overview, *Bull. Seismol. Soc. Am., 75,* 211-221, 1985.

Ponko, S. C., and C. O. Sanders, Inversion for P- and S-wave attenuation structure, Long Valley caldera, California, *J. Geophys. Res., 99,* 2619-2635, 1994.

Romero, A. E., T. V. McEvilly, E. L. Majer, and A. Michelini, Velocity Structure of the Long Valley Caldera from the Inversion of Local Earthquake P and S Travel Times, *J. Geophys. Res., 98,* 19869-19879, 1993.

Romero, A. E., T. V. McEvilly, E. L. Majer, and D. W. Vasco, Characterization of the geothermal system beneath the Northwest Geysers Steam Field, California, from seismicity and velocity pattern, *Geothermics, 24,* 471-487, 1995.

Rundel, J. B., and J. H. Whitcomb, A model for deformation in Long Valley caldera, California, 1980-1984, *J. Geophys. Res., 89,* 9371-9380, 1984.

Ryall, F., and A. Ryall, Attenuation of P and S waves in a magma chamber in Long Valley caldera, California, *Geophys. Res. Lett., 8,* 557-560, 1981.

Sanders, C. O., Location and configuration of magma bodies beneath Long Valley, California, determined from anomalous earthquake signals, *J. Geophys. Res., 89,* 8287-8302, 1984.

Sanders, C. O., Local earthquake tomography: attenuation theory and results, *Seismic Tomorgraphy: Theory and Practice,* Iyer, H. M., and K. Hirana (eds.). Chapman and Hall, London, 676-694, 1993.

Savage, J. C., R. S. Cockerham, J. E. Estrem, and L. R. Moore, Deformation near the Long Valley caldera, eastern California, 1982-1986, *J. Geophys. Res., 92,* 2721-2746, 1987.

Savage, J. C., and R. S. Cockerham, Earthquake swarm in Long Valley caldera, California, January 1983: Evidence for dike like inflation, *J. Geophys. Res., 89,* 8315-8324, 1984.

Sorey, M. L., G. A. Suemnicht, N. C. Sturchio, and G. A. Nordquist, New evidence on the geothermal system in Long Valley, California, from wells, fluid sampling, electrical geophysics, and Age determinations of hot-spring deposits, *J. Volc. Geoth. Res., 48,* 229-263, 1991.

Steck, L. K., and W. A. Prothero Jr., A 3-D raytracer for teleseimic body-wave arrival times, *Bull. Seismol. Soc. Am., 81,* 1332-1339, 1991.

Toksöz, M. N., C. H. Cheng, and A. Timur, Velocities of seismic waves in porous rocks, *Geophysics, 41,* 621-645, 1976.

Vasco, D. W., L. R. Johnson, and N. E. Goldstein, Using surface displacement and strain observations to determine deformation at depth, with application to Long Valley caldera, Calofirnia, *J. Geophys. Res., 93,* 3232-3242, 1988.

Zucca J. J., P. W. Kasameyer, J. M. Mills Jr., Observations of a reflection from the base of a magma chamber in Long Valley caldera, California, *Bull Seimol. Soc. Am., 77,* 1674-1687, 1987.

This preprint was prepared with the AGU LaTeX macros v3.0. File lvc.paper formatted 1999 June 28.

Figure 1. Simplified geological map of Long Valley region adopted from *Bailey et al.,* [1976]. The caldera boundary is represented by the dotted line. **X** marks the location of the DOE Exploratory Well; RD, resurgent dome; MM, Mammoth Mountain; CD, Casa Diabolo; HCF, Hilton Creek Fault; RVF, Round Valley Fault; VT, Volcanic Tableland. The near offset source was located at a distance of 165 m N65°E relative to the well, while the far offset source was at 1524 m N180°S. Because of scaling reasons both source locations are not indicated in the map.

Figure 2. Processing flow for the seismic data analysis.

Figure 3. a) Typical unedited data showing 10 groups of the three geophone components and the source sweep at a depth of 2075 m, b) Stacked, correlated, and rotated data for the three components of the geophone. In the coordinate system of the ray path, these components correspond to radial (component 1), in-plane normal (component 2), and out-of-plane normal (component 3). Note the different waves distinguished by their moveout velocity: P, direct P-wave; S, direct S-wave; T, tube wave.

Figure 4. a) P- and S-wave velocities averaged over 300m depth intervals. b) Poison's ratio determined from the velocities in 4a).

Figure 5. a) Near offset VSP-CDP map of P-wave reflections. b) Near offset VSP-CDP map of S-wave reflections.

Figure 6. Geologic cross section across the resurgent dome showing lithological units and faults (top), and map view indicating the location of the crossection within LVC (bottom). **X** indicates the location of the DOE Exploratory Well. Qef-rhyolitic flows and domes, Qet-rhyolite, Qbt-Bishop tuff, Pzms-metasedimentary rocks; (adopted from *Bailey,* [1989]).

Figure 7. F-K filtered seismograms, emphasising the reflected energy for a total travel time of 6 s. A coherent reflection is enhanced in the right panel below a travel time of 1.5 s.

Table 1. Summary of the VSP Data Acquisition

Offset [m]	Azimuth [°]	Acquired Depth [m]	Depth Interval [m]
165	65	550 - 2075	15
1524	180	1005 - 2075	15

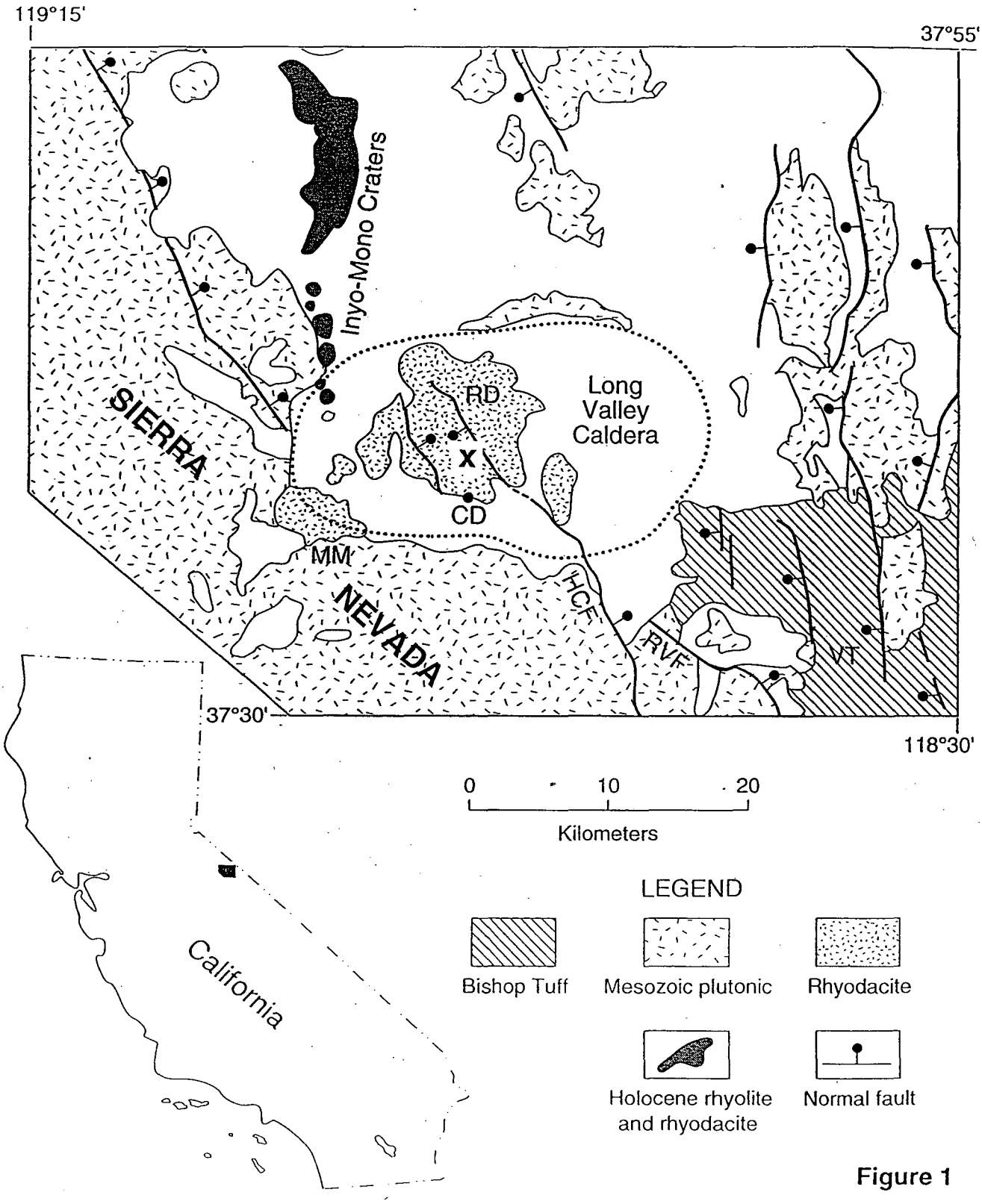
119°15'
37°55'
Inyo-Mono Craters
SIERRA
NEVADA
RD
X
CD
Long
Valley
Caldera
MM
HCF
RVF
VT
37°30'
118°30'
0
10
20
Kilometers
California
LEGEND
Bishop Tuff
Mesozoic plutonic
Rhyodacite
Holocene rhyolite
and rhyodacite
Normal fault

Figure 1

Flow Chart

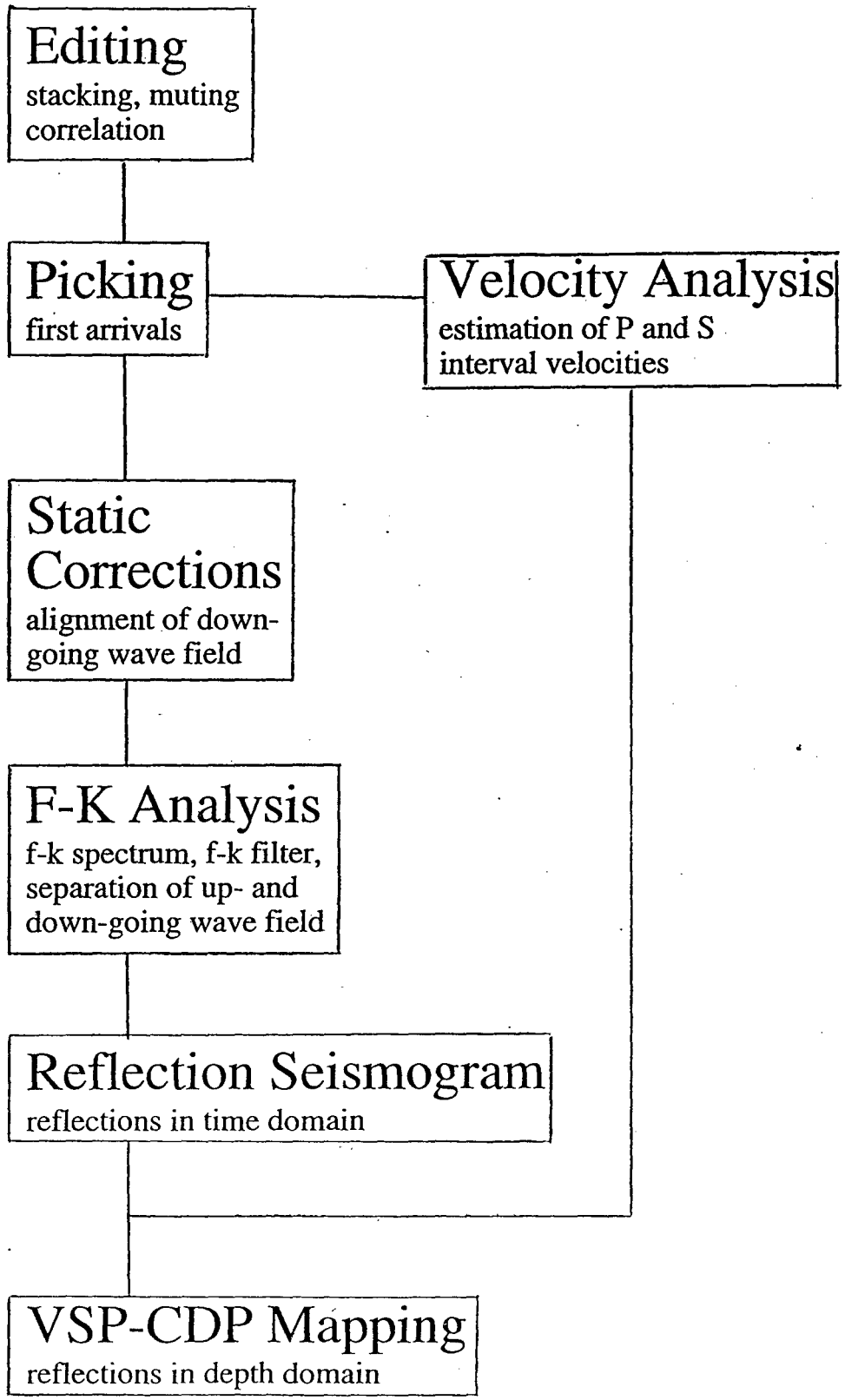

Figure 2

a)

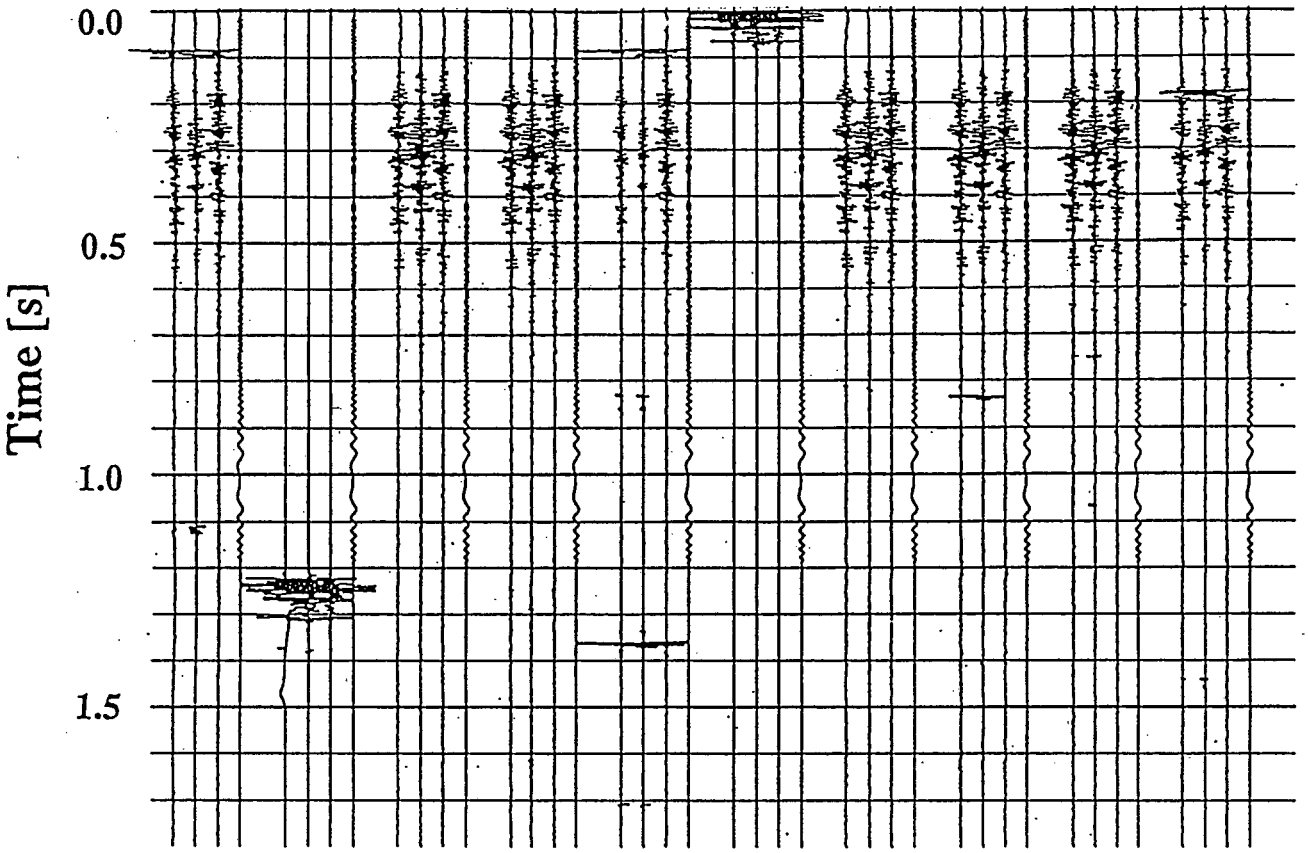

Figure 3a

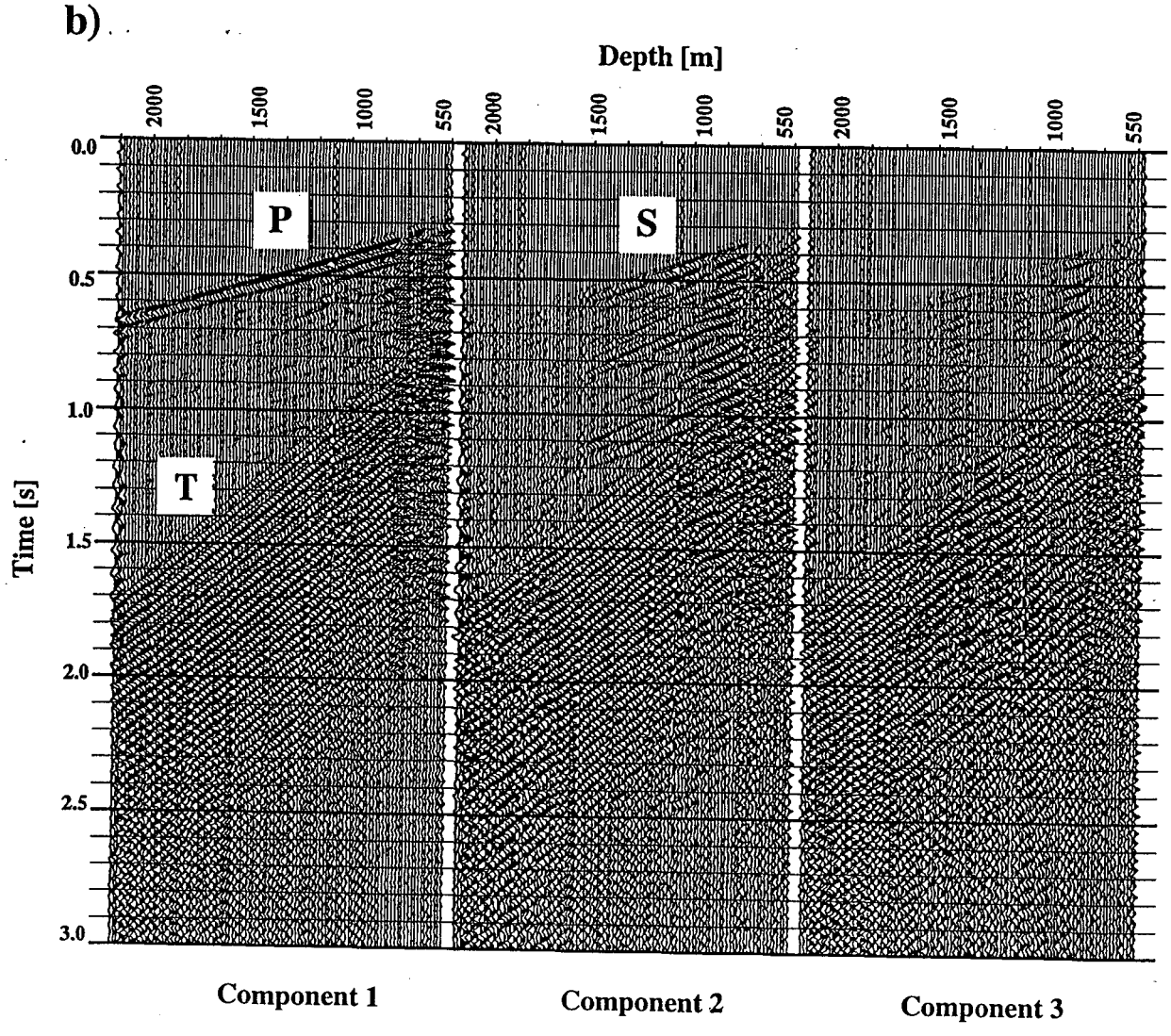
b)
Depth [m]
2000
1500
1000
550
0.0
0.5
1.0
1.5
2.0
2.5
3.0
Time [s]
P
S
T
Component 1
Component 2
Component 3

Figure 3b

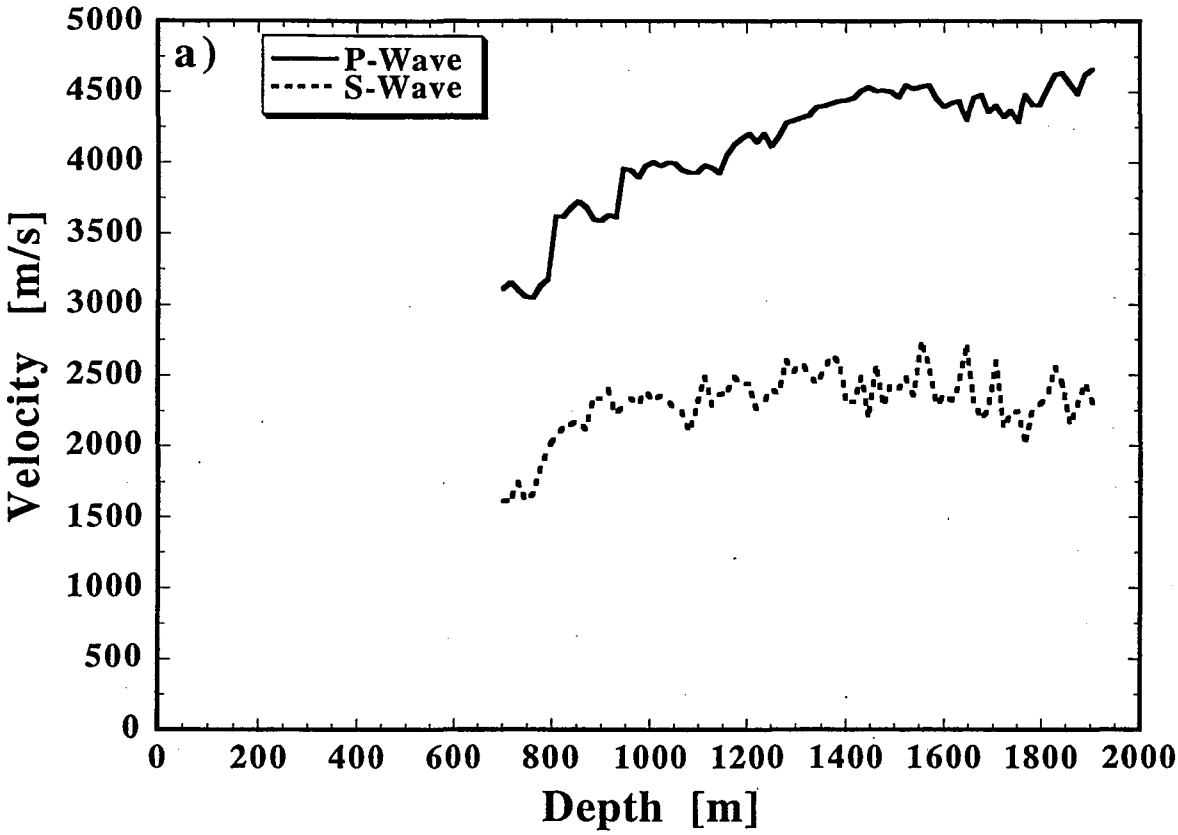
a)
P-Wave
S-Wave
Velocity [m/s]
5000
4500
4000
3500
3000
2500
2000
1500
1000
500
0
0
200
400
600
800
1000
1200
1400
1600
1800
2000
Depth [m]

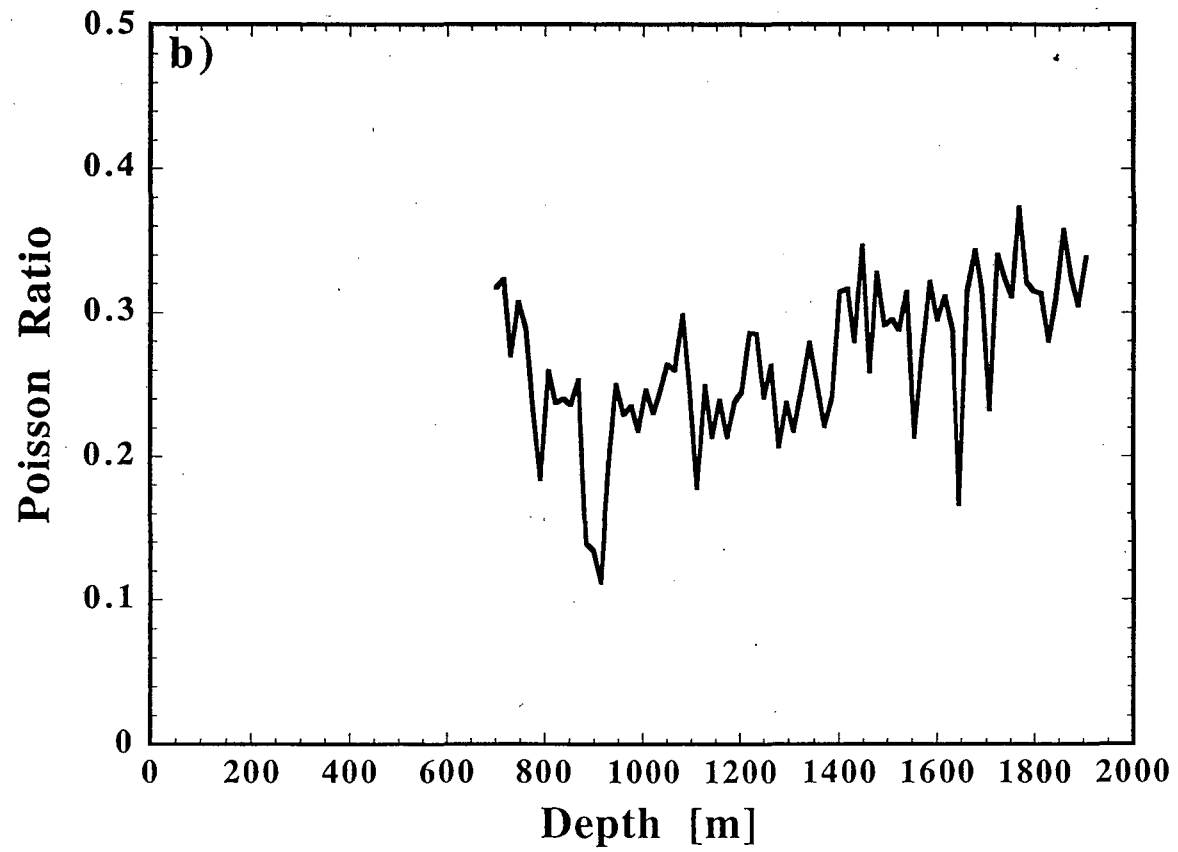
b)
Poisson Ratio
0.5
0.4
0.3
0.2
0.1
0
0
200
400
600
800
1000
1200
1400
1600
1800
2000
Depth [m]

Figure

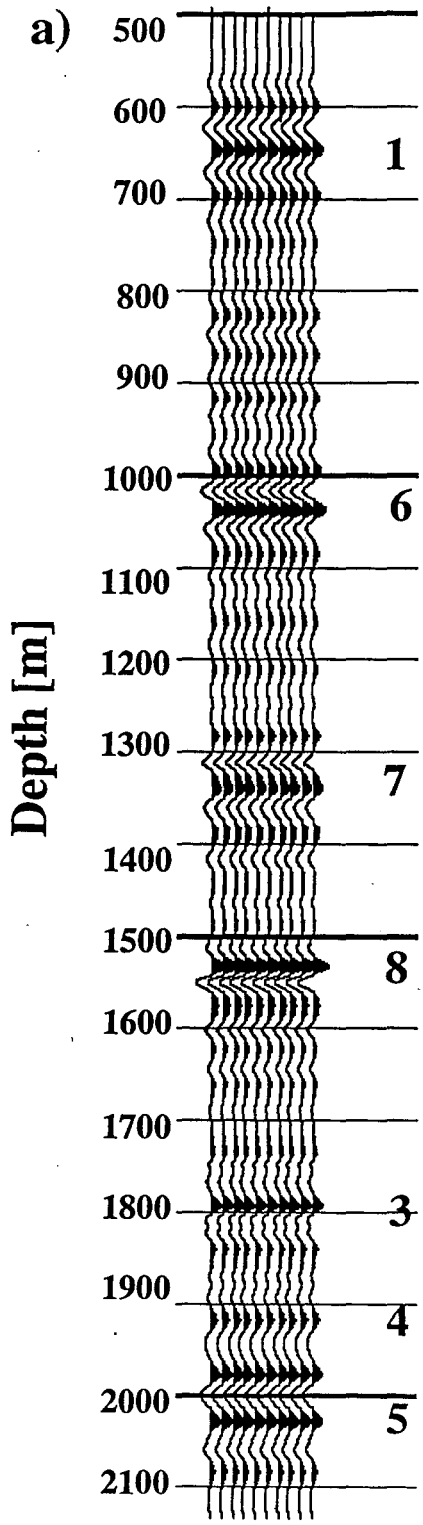
a)
Depth [m]
500
600
700
800
900
1000
1100
1200
1300
1400
1500
1600
1700
1800
1900
2000
2100
1
6
7
8
3
4
5

Figure 5a

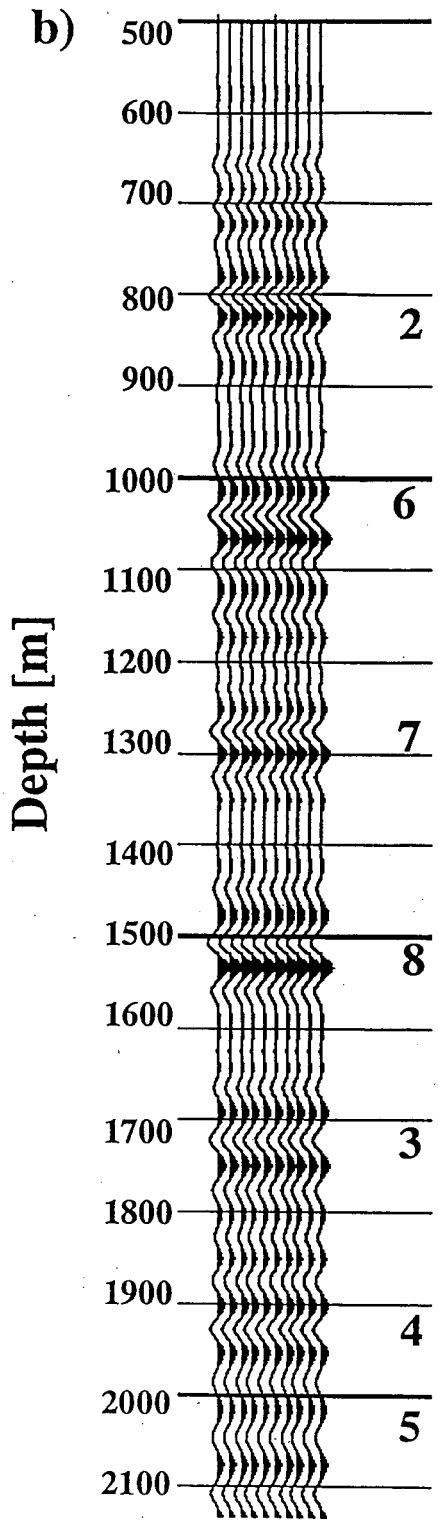
b)
Depth [m]
500
600
700
800
900
1000
1100
1200
1300
1400
1500
1600
1700
1800
1900
2000
2100
2
6
7
8
3
4
5

Figure 5

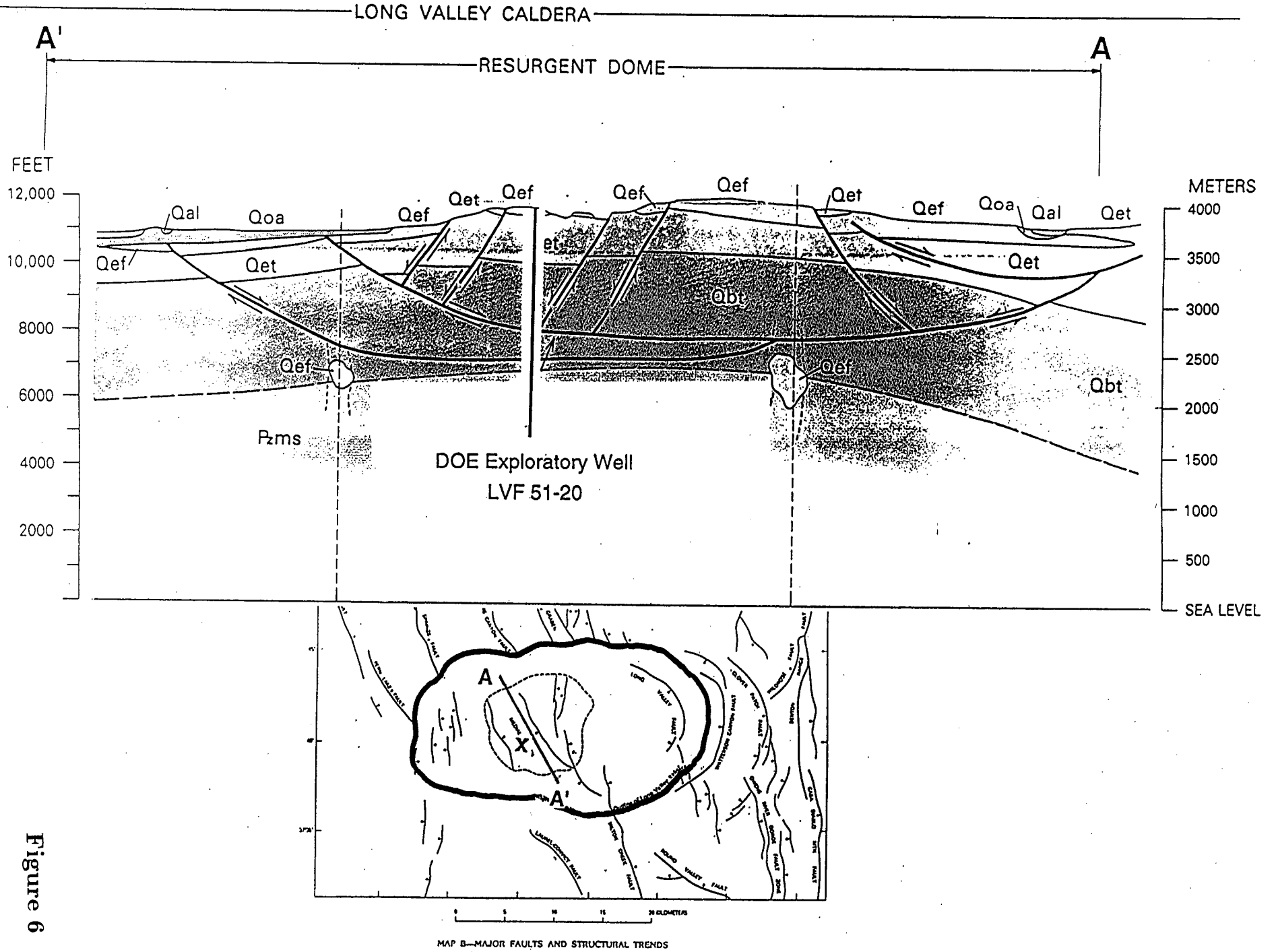
LONG VALLEY CALDERA
A'
A
RESURGENT DOME
FEET
12,000
10,000
8000
6000
4000
2000
METERS
4000
3500
3000
2500
2000
1500
1000
500
SEA LEVEL
Qal
Qoa
Qef
Qet
Qbt
Pzms
DOE Exploratory Well
LVF 51-20
MAP B—MAJOR FAULTS AND STRUCTURAL TRENDS

Figure 6

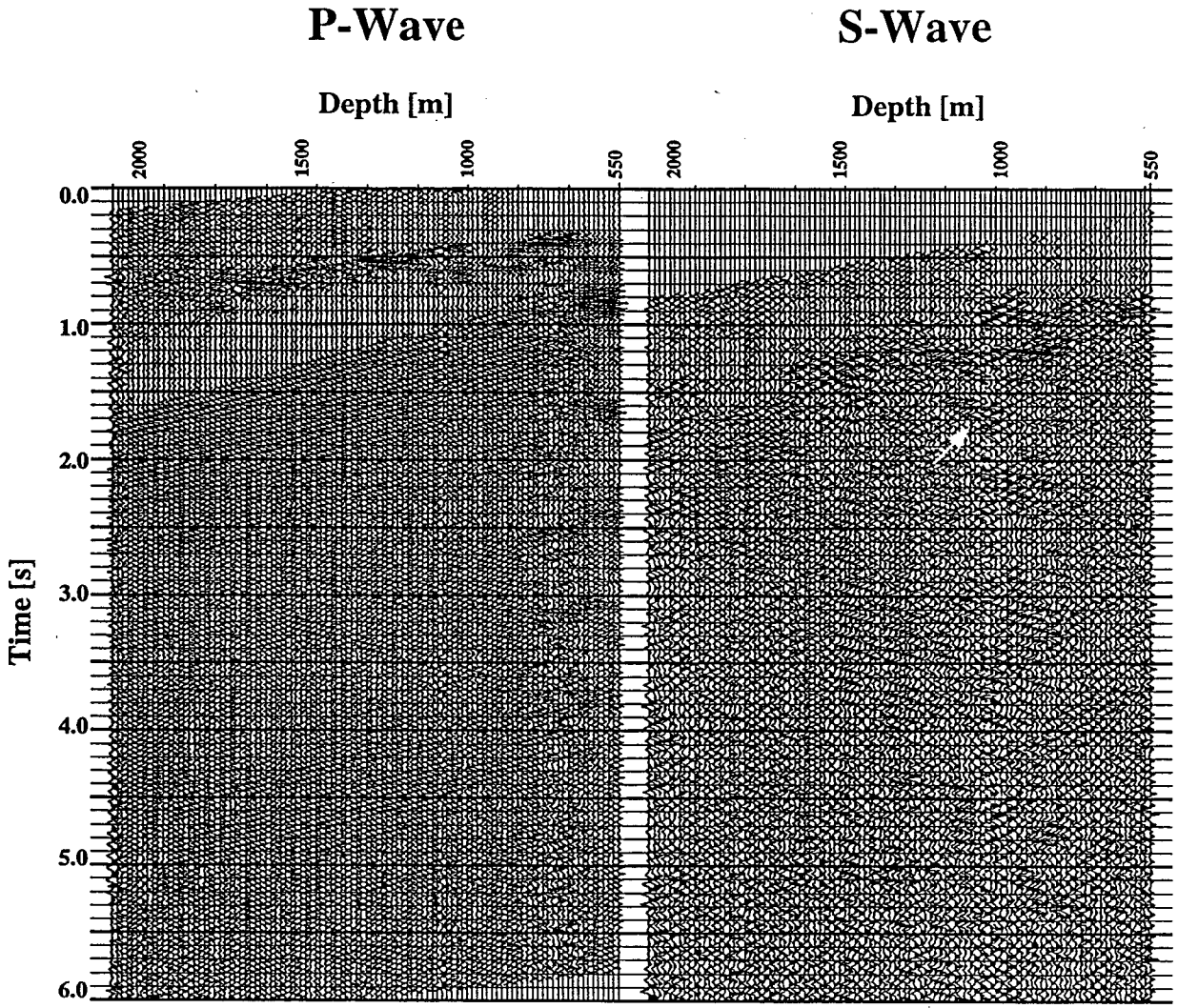
P-Wave
S-Wave
Depth [m]
Depth [m]
2000
1500
1000
550
2000
1500
1000
550
Time [s]
0.0
1.0
2.0
3.0
4.0
5.0
6.0

Figure 7

ERNEST ORLANDO LAWRENCE BERKELEY NATIONAL LABORATORY
ONE CYCLOTRON ROAD | BERKELEY, CALIFORNIA 94720

Prepared for the U.S. Department of Energy under Contract No. DE-AC03-76SF00098